For Polymer as an Article

Synthesis of Highly Conjugated Poly(3,9-carbazolyleneethynylenearylene)s Emitting Variously Colored Fluorescence

Kosaku Tamura,[†] Masashi Shiotsuki,[†] Norihisa Kobayashi,[‡] Toshio Masuda,[§] Fumio Sanda*,[†]

[†] *Department of Polymer Chemistry, Graduate School of Engineering, Kyoto University, Katsura Campus, Nishikyo-ku, Kyoto 615-8510, Japan*

[‡] *Department of Information and Image Sciences, Chiba University, Inage-ku, Chiba 263-8522, Japan*

[§] *Department of Environmental and Biological Chemistry, Faculty of Engineering, Fukui University of Technology, 3-6-1 Gakuen, Fukui 910-8505, Japan*

***** Correspondence author. Tel.:+81 75 383 2591; fax +81 75 383 2592. E-mail address: sanda@adv.polym.kyoto-u.ac.jp

ABSTRACT: Novel conjugated polymers **P1**–**P7** containing 3,9-linked carbazole units in the main chain were synthesized by the polycondensation of 3-ethynyl-9-(4-ethynylphenyl)carbazole (EEPCz) and dihaloarenes, and their optical and electrical properties were studied. Polymers with weight-average molecular weights of 4100–48 000 were obtained in 24–92% yields by the Sonogashira coupling polycondensation in tetrahydrofuran (THF)/Et_3N at 30 or 50 °C for 48 h. All the polymers absorbed light around 350 nm. The polymers with electron-accepter units exhibited absorption bands originating from charge transfer. The polymers except the one containing azobenzenes emitted variously colored fluorescence with moderate quantum yields upon excitation at the absorption maxima. **P1**–**P3** were oxidized around 0.6 V, and then reduced around 0.5 V. The conductivity of **P3** was 1.1×10^{-14} S/cm at 10^3 V/cm.

Keywords: carbazole, conjugated polymer, fluorescence

1. Introduction

Carbazole is a well-known conjugated unit that has interesting optical and electronic properties such as photoconductivity and photorefractivity [1]. Carbazole derivatives are used as materials for hole-transporting layers of electroluminescent devices due to their high charge mobility [2]. Carbazole derivatives are also usable to light-emitting layers because they are thermally stable and show blue photo- and electroluminescence based on the large band gap of the biphenyl unit and planarity improved by the bridging nitrogen atom [3]. Much effort has been done to synthesize polymers carrying carbazoles in the main chain, e.g., poly(carbazole) possessing carbazolylene main chain exhibits properties largely different from each other according to the position of linkage (Chart 1). The main-chain conjugation of 3,6-linked poly(carbazole)s is not long, because one-electron abstraction from the nitrogen atom forms stable cation radical species that disturb conjugation [4]. Compared to 3,6-linked poly(carbazole)s, the main chain conjugation of 2,7-linked poly(carbazole)s is long, because the main chain can form a resonance structure like poly(*p*-phenylene). In fact, 2,7-linked poly(carbazole)s emit blue light in the film state based on the long conjugation length [5].

Insert Chart 1 here

On the other hand, less attention has been paid to 3,9-carbazolylene-based conjugated polymers compared with 3,6- and 2,7-linked ones, presumably due to their difficult synthesis.

A few examples are 3,9-poly(carbazole) [6] and 3,9-linked copolymers of carbazole with fluorine [7]. Since conjugated polymers containing 3,9-linked carbazole have C–N bond in the main chain, it is interesting to investigate the effect of unshared electron pair of the nitrogen atom on the optical properties and the redox reaction of the polymers. 3,9-Carbazolylene-based polymers are expected to be applicable to light emitting layers, because the conjugation of the main chain seems to be extended through nitrogen atom.

Meanwhile, poly(aryleneethynylene) is also a typical conjugated polymer that possesses photo-electronic properties. Especially, it strongly emits fluorescence due to the rigid structure that reduces nonradiative decay [8]. Some poly(aryleneethynylene)s feature almost quantitative fluorescence quantum yields [9]. Poly(aryleneethynylene)s containing carbazole in the main chain emit intense blue–green fluorescence in high quantum yields [10].

We have recently synthesized 3,9- and 2,9-linked carbazole-containing conjugated polymers including poly(3,9-carbazolyleneethynylenephenylene) (Chart 2) by the polycondensation of ethynyl- and iodo-substituted 9-arylenecarbazolylene monomers, and examined the optical and electrical properties [11]. The polymers absorbed light at wavelength regions longer than those of the corresponding monomers due to the conjugated main chain through the nitrogen atom of the carbazole unit. The drawback of the polymers was poor solubility. Solvent-soluble polymers are desirable from the viewpoint of assembling photoelectric devices. In this paper, we report the synthesis of 3,9-linked

carbazole-containing conjugated novel polymers **P1**–**P7** by the polycondensation of 3-ethynyl-9-(4-ethynylphenyl)carbazole (EEPCz) with dihaloarenes **1**–**7** (Scheme 1), and examination of the optical and electrical properties, along with the analogous polymer **P3'**.

Insert Chart 2 here

Insert Scheme 1 here

2. Experimental Section

Measurements. ^{1}H (400 MHz) and ^{13}C (100 MHz) NMR spectra were recorded on a JEOL EX-400 spectrometer using tetramethylsilane as an internal standard. IR, UV-vis and fluorescence spectra were measured on JASCO FT/IR-4100, V-550 and FP-750 spectrophotometers, respectively. Cyclic voltammograms (CV) were recorded with an HCH Instruments ALS600A-n electrochemical analyzer. Melting points (mp) were measured on a Yanaco micro melting point apparatus. Elemental analysis was done at the Microanalytical Center of Kyoto University. Mass spectra were measured on a JEOL JMS-HX110A mass spectrometer. Number- and weight-average molecular weights (M_n and M_w) of polymers were determined by gel permeation chromatography (GPC) on a JASCO GULLIVER system (PU-980, CO-965, RI-930, and UV-1570) equipped with polystyrene gel columns (Shodex columns K805 × 3), using THF as an eluent at a flow rate of 1.0 mL/min, calibrated by polystyrene standards at 40 °C.

Materials. Unless otherwise stated, reagents were commercially obtained, and used without further purification. 3-(Trimethylsilylethynyl)carbazole [12], 9-(4-iodophenyl)-3-trimethylsilylethynylcarbazole [11], 4,4'-diiodoazobenzene (**4**) [13], 4,7-dibromo-2,1,3-benzothiadiazole (**6**) [14] and 4,7-bis(5-bromo-2-thienyl)-2,1,3-benzothiadiazole (**7**) [15] were synthesized according to the literature. The solvents used for polycondensation were purified before use by the standard methods.

EEPCz. Trimethylsilylacetylene (1.13 mL, 8.00 mmol) was added to a mixture of 9-(4-iodophenyl)-3-trimethylsilylethynylcarbazole (1.88 g, 4.04 mmol), $PdCl_2(PPh_3)_2$ (28.0 mg, 0.0399 mmol), PPh_3 (31.0 mg, 0.118 mmol), CuI (30.0 mg, 0.157 mmol) and Et_3N (30 mL) under hydrogen, and the resulting mixture was stirred at room temperature overnight. Then, solvent-insoluble salt precipitated was filtered off, and Et_3N was removed from the mixture by evaporation. The residue was extracted with $CHCl_3$, and the combined organic layer was washed with 1 M HCl, sat. $NaHCO_3$ aq. and water. The organic layer was dried with anhydrous $MgSO_4$, and concentrated by evaporation to give brown solid. It was purified by silica gel column chromatography eluted with hexane/ethyl acetate to obtain 3-trimethylsilylethynyl-9-(4-trimethylsilylethynylphenyl)carbazole as white solid. After that, it was dissolved in THF (45 mL), and a suspension of K_2CO_3 (1.17 g, 8.47 mmol) and MeOH (75 mL) was added to the solution. The resulting mixture was stirred at room temperature

overnight. The solution was extracted with ethyl acetate, and the combined organic layer was washed with water subsequently, dried over anhydrous $MgSO_4$, and concentrated on a rotary evaporator to give pale yellow solid. It was purified by silica gel column chromatography eluted with hexane/ethyl acetate to obtain EEPCz as white solid. Yield: 0.589 g (2.02 mmol, 54%). Mp: 115.2–116.2 °C. ^{1}H NMR (400 MHz, ppm, $CDCl_3$): 3.08 (s, 1H, -C≡CH), 3.18 (s, 1H, -C≡CH), 7.27–7.34 (m, 2H, Ar), 7.36–7.45 (m, 2H, Ar), 7.47–7.55 (m, 3H, Ar), 7.71 (d, J = 8.3 Hz, 2H, Ar), 8.09 (d, J = 7.6 Hz, 1H, Ar), 8.28 (s, 1H, Ar); ^{13}C NMR (100 MHz, ppm, $CDCl_3$): 75.6 (-C≡*C*H), 78.4 (-C≡*C*H), 82.7 (-*C*≡CH), 84.6 (-*C*≡CH), 109.7, 109.9, 113.6, 120.5, 120.8, 122.9, 121.5, 123.0, 123.5, 124.6, 126.6, 126.8, 130.0, 133.7, 137.5, 140.3, 140.9. IR (cm^{-1}, KBr): 3276 (H–C≡), 3044, 2100 (HC≡C), 1600, 1512, 1485, 1475, 1455, 1361 (N–Ar), 1327, 1281, 1226, 1188, 1105, 848, 839, 806, 766, 744, 727, 669, 641, 629, 601, 591, 417. Anal. Calcd for $C_{22}H_{13}N$: C 90.69; H 4.50; N 4.81. Found: C 90.79; H 4.60; N 4.62.

1,4-Bis(3-ethynyl-9-carbazolyl)benzene (8). A mixture of 3-(trimethylsilylethynyl)carbazole (0.50 g, 1.90 mmol), 1,4-diiodobenzene (0.30 g, 0.94 mmol), CuI (19.1 mg, 0.10 mmol), 1,10-phenanthroline (68.5 mg, 0.38 mmol), K_3PO_4 (0.81 g, 3.82 mmol), and toluene (15 mL) was stirred at 120 °C for 24 h. After cooling, the residue was extracted with CH_2Cl_2, and the organic layer was combined and washed with water. The organic layer was dried with anhydrous $MgSO_4$, and concentrated on a rotary evaporator

to give gray solid. It was purified by silica gel column chromatography eluted with hexane/ethyl acetate to obtain 1,4-bis(3-trimethylsilylethynyl-9-carbazolyl)benzene as white solid. After that, it was dissolved in THF (15 mL), and a suspension of K_2CO_3 (0.23 g, 1.90 mmol) and MeOH (15 mL) was added to the solution and the resulting mixture was stirred at room temperature overnight. The solution was extracted with ethyl acetate, and the combined organic layer was washed with water subsequently, dried over anhydrous $MgSO_4$, and concentrated on a rotary evaporator to give pale yellow solid. It was purified by silica gel column chromatography eluted with hexane/ethyl acetate to obtain **8** as white solid. Yield: 0.18 g (0.39 mmol, 40%). Mp: 204.7–205.7 °C; ^{1}H NMR (400 MHz, ppm, $CDCl_3$): 3.11 (s, 2H, -C≡CH), 7.36 (vt, *J* = 7.3 Hz, 2H, Ar), 7.46–7.53 (m, 4H, Ar), 7.55 (d, *J* = 8.0 Hz, 2H, Ar), 7.60 (d, *J* = 8.5 Hz, 2H, Ar), 7.81 (s, 4H, Ar), 8.16 (d, *J* = 7.8 Hz, 2H, Ar), 8.34 (s, 1H, Ar); ^{13}C NMR (100 MHz, ppm, $CDCl_3$): 75.7 (-C≡*C*H), 84.7 (-*C*≡CH), 109.7, 109.9, 113.6, 120.6, 120.9, 123.0, 123.5, 124.7, 126.7, 128.4, 130.1, 136.5, 140.5, 141.1. IR (cm^{-1}, KBr): 3309 (H–C≡), 3043, 2919, 2109 (HC≡C), 1517, 1475, 1452, 1352 (N–Ar), 1325, 1230, 1184, 1105, 807, 766, 742, 727, 651, 630, 592, 570, 504, 419. Anal. Calcd for $C_{34}H_{20}N_2$: C 89.45; H 4.42; N 6.14. Found: C 89.26; H 4.72; N 6.05.

Polycondensation. All the polycondensations were carried out in a glass tube equipped with a three-way stopcock under nitrogen. A monomer (0.25 mmol) solution was added to a catalyst solution under dry nitrogen, and the resulting solution was kept at 30 or

50 °C for 48 h. To the reaction mixture, 1 M HCl aq. (5.0 mL) was added, and the resulting mixture was poured into MeOH (300 mL) to precipitate a polymer. It was separated from the supernatant by filtration. THF (5–20 mL) was added to the polymer, and the resulting mixture was filtered. The filtrate was poured into MeOH (300 mL) to precipitate a polymer once again. It was separated from the supernatant by filtration and dried under reduced pressure.

Spectroscopic Data of the Polymers. **P1** ^{1}H NMR (400 MHz, ppm, $CDCl_3$): 7.3–7.4 (br, 6H, Ar) 7.5–7.6 (br, 5H, Ar) 7.7–7.8 (br, 2H, Ar) 8.1–8.2 (br, 1H, Ar) 8.3–8.4 (br, 1H, Ar). IR (cm^{-1}, KBr): 3041, 2919, 2850, 2210 (C≡C), 1599, 1515, 1487, 1474, 1454, 1362 (N–Ar), 1227, 1004, 835, 807, 743. **P2** ^{1}H NMR (400 MHz, ppm, $CDCl_3$): 7.3–7.4 (br, 6H, Ar) 7.5–7.6 (br, 5H, Ar) 7.7–7.8 (br, 2H, Ar) 8.1–8.2 (br, 1H, Ar) 8.3–8.4 (br, 1H, Ar). IR (cm^{-1}, KBr): 3045, 2960, 2207 (C≡C), 1590, 1512, 1484, 1454, 1362 (N–Ar), 1226, 806, 744. **P3** ^{1}H NMR (400 MHz, ppm, $CDCl_3$): 0.8–0.9 (br, 6H, -$CH_2C\mathit{H_3}$), 1.1–1.5 (br, 20H, -CH_2-), 1.7–1.9 (br, 4H, -CH_2-), 2.8–2.9 (br, 4H, -CH_2-), 7.3–7.4 (br, 1H, Ar) 7.4–7.5 (br, 5H, Ar) 7.5–7.6 (br, 3H, Ar) 7.7–7.8 (br, 2H, Ar) 8.1–8.2 (br, 1H, Ar) 8.3–8.4 (br, 1H, Ar). IR (cm^{-1}, KBr): 2922, 2852, 2200 (C≡C), 1514, 1361 (N–Ar), 1227, 1103, 807, 743. **P4** ^{1}H NMR (400 MHz, ppm, $CDCl_3$): 7.3–7.4 (br, 1H, Ar) 7.4–7.5 (br, 4H, Ar) 7.6–7.8 (br, 6H, Ar) 7.8–7.9 (br, 3H, Ar) 7.9–8.0 (br, 3H, Ar) 8.1–8.2 (br, 1H, Ar) 8.3–8.4 (br, 1H, Ar). IR (cm^{-1}, KBr): 3042, 2958, 2922, 2852, 2204 (C≡C), 1513, 1474, 1454, 1361 (N–Ar), 1325, 1226,

1098, 1003,844, 806, 743. **P5** ^{1}H NMR (400 MHz, ppm, $CDCl_3$): 7.3–7.6 (br, 8H, Ar) 7.6–7.9 (br, 7H, Ar) 8.0–8.3 (br, 2H, Ar) 8.5–8.6 (br, 1H, Ar) 8.7–8.8 (br, 1H, Ar). IR (cm^{-1}, KBr): 3042, 2917, 2850, 2199 (C≡C), 1597, 1510, 1475, 1455, 1360 (N–Ar), 1325, 1228, 743, 419, 404. **P6** ^{1}H NMR (400 MHz, ppm, $CDCl_3$): 7.3–7.4 (br, 1H, Ar) 7.4–7.5 (br, 3H, Ar) 7.6–7.8 (br, 4H, Ar) 7.8–8.0 (br, 3H, Ar) 8.1–8.2 (br, 1H, Ar) 8.4–8.5 (br, 1H, Ar). IR (cm^{-1}, KBr): 3291, 3043, 2961, 2916, 2203 (C≡C), 1598, 1509, 1474, 1454, 1362 (N–Ar), 1326, 1228, 837, 808, 744. **P7** ^{1}H NMR (400 MHz, ppm, $CDCl_3$): 7.1–7.2 (br, 1H, Ar) 7.3–7.4 (br, 1H, Ar) 7.4–7.5 (br, 3H, Ar) 7.6–7.8 (br, 2H, Ar) 7.8–7.9 (br, 4H, Ar) 7.9–8.0 (br, 2H, Ar) 8.0–8.1 (br, 1H, Ar) 8.1–8.2 (br, 2H, Ar) 8.3–8.4 (br, 1H, Ar). IR (cm^{-1}, KBr): 3289, 3045, 2961, 2872, 2200 (C≡C), 1598, 1509, 1475, 1454, 1362 (N–Ar), 1326, 1229, 1065, 807, 746. **P3'** ^{1}H NMR (400 MHz, ppm, $CDCl_3$): 0.8–0.9 (br, 6H, -$CH_2C\mathit{H_3}$), 1.1–1.5 (br, 20H, -CH_2-), 1.7–1.9 (br, 4H, -CH_2-), 2.8–2.9 (br, 4H, -CH_2-), 7.3–7.4 (br, 2H, Ar) 7.4–7.6 (br, 8H, Ar) 7.6–7.7 (br, 4H, Ar) 7.8–7.9 (br, 4H, Ar) 8.1–8.2 (br, 2H, Ar) 8.3–8.4 (br, 2H, Ar). IR (cm^{-1}, KBr): 3041, 2922, 2851, 2201 (C≡C), 1516, 1475, 1453, 1351 (N–Ar), 1324, 1227, 806, 743.

Evaluation of Photoconductivity. A 2 wt % solution of **P3** in THF was cast on an ITO electrode and then dried in vacuo for 12 h to prepare a thin film with a thickness of 20 μm. Au was vacuum-evaporated to prepare a counter electrode for the ITO electrode. The relationships between current (I) and applied voltage (V) for the ITO/**P3**film/Au cells (effective electrode area 0.12 cm^2) were measured at room temperature under reduced

pressure of 10^{-2} Torr in the dark and under photo-illumination (2.5 mW/m^2) with a Xe lamp using a thermoabsorption filter.

Molecular Mechanics and Molecular Orbital Calculations. The geometries of the conformers in Figure 4 were optimized first with molecular mechanics using the MMFF94 force field [16], then with the semiempirical molecular orbital method using the AM1 hamiltonian on Wavefunction, Spartan '06 Windows. The ends of the trimers were terminated with methyl groups. The UV-vis spectra of EEPCz and **P1**–**P3** were predicted regarding EEPCz and the trimers of **1**–**3** using the MOS-F, ZINDO [17] on Fujitsu Scigress Explorer 7.7, wherein the geometries were optimized using the AM1.

3. Results and Discussion

3.1 Monomer Synthesis. Scheme 2 illustrates the synthetic routes for carbazole-based monomers EEPCz and **8** having two ethynyl groups. EEPCz was synthesized by the Sonogashira coupling of 9-(4-iodophenyl)-3-trimethylsilylethynylcarbazole with trimethylsilylacetylene, followed by desilylation using K_2CO_3 [12]. Monomer **8** was synthesized by the Ullmann type coupling of diiodobenzene with two equivalents of 3-trimethylsilylethynylcarbazole, followed by desilylation. The monomers were obtained as white solids after purification by column chromatography. The structures of the monomers were confirmed by ^{1}H, ^{13}C NMR, and IR spectroscopies besides elemental analysis.

Insert Scheme 2 here

3.2 Polycondensation. Table 1 summarizes the conditions and results of the polycondensation of carbazole-based EEPCz with diharoarenes **1**–**7** catalyzed with $PdCl_2(PPh_3)_2$–CuI in THF/Et_3N at 30 or 50 °C for 48 h. Diiodoarenes **1**–**4** gave polymers with M_w = 4100–48 000 in moderate yields (57–92%). On the other hand, dibromoarenes **5**–**7** gave polymers with M_w = 7 900–9 600 in low yields (24–31%). This difference seems to be caused by the reactivity of bromoarenes lower than that of iodoarenes in the Sonogashira coupling reaction [18]. The formed polymers exhibited niether ^{1}H NMR signals at 3.08 and 3.18 ppm, nor IR absorption peak at 3276 cm^{-1} due to the ethynyl groups of EEPCz. In addition, carbazole-based diethynyl monomer **8** and diiodoarene **3** were polymerized to give the corresponding polymer **P3'** with M_w = 4 100, M_w/M_n = 4.0 in 30% yield. **P3'** did not exhibit the ^{1}H NMR signal and IR absorption peak due to the ethynyl group of **8**, either. In the synthesis of **P4**–**P7** and **P3'**, THF-insoluble parts were partly formed. It was considered that the THF-insoluble parts were high-molecular-weight polymers because the IR spectra were almost the same as those of the THF-soluble parts. Table 2 summarizes the solubility of THF-soluble parts of the polymers and poly(3,9-carbazolyleneethynylenephenylene) (Chart 2). All the polymers were also soluble in $CHCl_3$. **P1** and **P2** were soluble in toluene, CH_2Cl_2 and DMF in addition to $CHCl_3$ and

THF. Their solubility was high compared with poly(3,9-carbazolyleneethynylenephenylene) (Chart 2). **P3** was partly soluble in hexane, indicating that the octyl side chains enhanced the lipophilicity.

Insert Table 1 here

Insert Table 2 here

3.3 Optical Properties. Figure 1 shows the UV-vis spectra of EEPCz and **P1**–**P7** measured in THF. **P1**–**P4** exhibited carbazole-based absorption peaks around 300 nm, and also around 350 nm that was not observed in the spectra of EEPCz. This fact indicates the existence of main chain conjugation via nitrogen atom of the carbazole unit. The absorption peak of **P2** was positioned at a wavelength shorter than those of **P1**, presumably due to the *meta*-phenylene structure, which is unfavorable for conjugation compared to the *para*-linked one. **P5**–**P7** also exhibited carbazole-based absorption peaks around 300 nm, and absorption bands over 400 nm originating from intramolecular charge transfer [19].

Insert Figure 1 here

Figure 2 shows the UV-vis spectra of **8** and **P3'** measured in THF. The λ_{max} of **P3'** was positioned at 341 nm, 70 nm longer than that of **8**, indicating that **P3'** is largely conjugated compared with **8**. It should be noted that the λ_{max} of **P3'** was a little shorter than that of **P3**. It seems that the carbazole units and phenylene spacer of **8** are twisted due to the

repulsion between the 1,8-protons of carbazole and phenylene protons, leading to the conjugation length of **P3'** shorter than that of **P3**.

Insert Figure 2 here

Figure 3 illustrates the UV-vis spectra of **P1** and **P2** predicted by the MOS-F (ZINDO) method [17], together with the relationship between the predicted and observed λ_{max} values of EEPCz and **P1**–**P3**. Trimers were used for prediction of **P1**–**P3**, wherein both ends were terminated with methyl groups. The λ_{max} of **P1** was predicted to be 325 nm, 30 nm shorter than the one observed. One possible reason for the deviation is the difference between the trimer (predicted) and polymer (observed). Neglect of solvent effects in calculation also seems to affect it [20]. EEPCz, **P2** and **P3** showed the same tendency. The almost linear relationship between the predicted and observed λ_{max} values indicates that the ZINDO can appropriately simulate the UV-vis absorption spectra of the polymers.

Insert Figure 3 here

The λ_{max} difference between **P1** and **P2** was about 15 nm both in the observed and predicted spectra. Semiempirical molecular orbital calculations of trimers of **P1** and **P2** were carried out using the AM1 hamiltonian to obtain the information on conjugation of the polymers. As shown in Figure 4, the HOMO of **P2**-trimer was extended over 1.5 units through *meta*-phenylene and two carbazole units. On the other hand, the HOMO of **P1**-trimer was largely extended over 2.5 units through two *para*-phenylene and three

carbazole units. It is understood that **P1** delocalizes the electron through the main chain more than **P2**, leading to the longer λ_{max}.

Insert Figure 4 here

Figure 5 depicts the fluorescence spectra of EEPCz, **8** and **P1**–**P7** excited at the main chain-based absorption maxima. Table 3 lists the fluorescence spectroscopic data of the polymers, along with the absorption λ_{max}. EEPCz emitted vibronic fluorescence due to the carbazole moiety around 360 nm. **P1**–**P7** emitted fluorescence at longer wavelength regions than EEPCz. **P1**–**P3** and **P3'** emitted blue fluorescence around 390–400 nm in quantum yields ranging from 61 to 91%, which are very high among poly(carbazolyleneethynylenearylene)s reported so far [10]. **P4** also emitted fluorescence at this region, but the quantum yield was very low (0.33%), presumably because of the isomerization of azobenzene moiety that will be described later. **P5**, **P6** and **P7** emitted green (499 nm), yellow (548 nm) and orange (566 nm) fluorescence, respectively. It is thought that charge transfer occurred from carbazole to accepter units, leading to the fluorescence emission at these long wavelength regions [19]. The relatively low quantum yields (22–28%) are attributable to this charge transfer.

Insert Figure 5 here

Insert Table 3 here

Figure 6 shows the UV-vis and fluorescence spectra of **P1** measured in various

solvents. The UV-vis spectral patterns were almost the same one another irrespective of the solvents. The fluorescence spectra showed similar shapes except in toluene. π-π Interaction between **P1** and toluene possibly caused this difference.

Insert Figure 6 here

Figure 7 shows the UV-vis and fluorescence spectra of **P3** fabricated in a film by casting a toluene solution on a quartz plate. There was little difference between the UV-vis spectra of the solution (Figure 1) and film samples. On the other hand, the **P3** film showed two kinds of fluorescence peaks, sharp one at 403 nm and broad one at a longer wavelength region, which was not observed in the **P3** solution (Figure 5b). The latter emission is attributable to excimers because π-stacking between polymer chains occurs largely in the bulk than in diluted solution [21].

Insert Figure 7 here

A **P4** solution in THF was irradiated with UV light at a wavelength of 300 nm < λ < 400 nm at 20 °C to check the isomerization of azobenzene unit, which was monitored by UV–vis absorption spectroscopy. As shown in Figure 8, **P4** strongly absorbed light around 350 nm, which is attributable to π–π* transition band of the conjugated main chain containing *trans*-azobenzene units. This absorption slightly decreased the intensity upon UV-light irradiation to level off in 1 min. Simultaneously, a weak shoulder absorption attributable to n–π* transition band of *cis*-azobenzene units appeared around 410 nm. These spectral

changes indicate that *trans*-to-*cis* photo-isomerization of azobenzene moieties took place at the polymer main chain. Next, the UV-light irradiated sample was further irradiated with visible light to check the reversibility of photo-isomerization of the azobenzene units. **P4** slightly increased and decreased the absorption around 350 and 410 nm upon visible-light irradiation, respectively. After 1 min, the UV–vis absorption returned to the original state. These spectral changes indicate the *cis*-to-t*rans* photo-isomerization of azobenzene moieties in the polymer, and the isomerization is reversible. It seems that the small degree of photo-isomerization is due to the overlap of absorption bands of azobenzene with those of conjugated main chain, which prevents the azobenzene moieties from efficient excitation by photo-irradiation.

Insert Figure 8 here

3.4 Electrochemical Properties. We further examined the electrochemical properties of the polymers. Figure 9 (a) depicts the CV curves of **P1** measured in CH_2Cl_2 with tetra-*n*-butylammonium perchlorate as an electrolyte and Ag/Ag^+ electrode as a reference. **P1** was reversibly oxidized at 0.52 V and then reduced at 0.47 V, which was likely to occur at nitrogen atom of carbazole unit. **P1** did not exhibit a peak based on the formation of C–C bond linkages between the 6-positioned carbons of carbazoles at adjacent polymer chains. It seems that cation radical generated by oxidation is delocalized to suppress this reaction.

Moreover, we investigated the relationship between oxidation voltage (E_{ox}) and λ_{max} of **P1**–**P3** together with EEPCz. As shown in Figure 9 (b), E_{ox} and λ_{max} showed a linear relationship. It is considered that a long conjugation length narrows the band gap, leading to a low E_{ox}.

Insert Figure 9 here

3.5 Conductivity. Figure 10 depicts the *I*–*V* curve of an ITO/**P3**/Au cell. The dark conductivity was calculated to be 1.1×10^{-14} S/cm under an electric field of 10^3 V/cm (2 V). This conductivity is 2 orders higher than that of a polyphenylacetylene carrying carbazole moieties in the side chain [22], presumably due to the π-conjugation of the main chain, which is effective for electronic functional applications. The current under an applied voltage at 2 V was twice as large under photo-illumination as in the dark. This proves that **P3** is photoconductive. It has been reported that photocurrent/dark current ratio of polyacetylenes carrying carbazole moieties in the side chain is 10–50 [22], which depends on the structure but is much larger than that of **P3**. As mentioned above, the present polymers showed fluorescence quantum yields higher than polyacetylenes with carbazole pendants, suggesting that quenching effectively diminishes photogenerated holes. It is assumed that **P3**, therefore, shows lower photoconductive properties. However, the results of Figure 10 clearly indicate that the designed polymer works as a photoelectronic functional polymer such as light-emitting materials.

Insert Figure 10 here

4. Summary

In this article, we have demonstrated the synthesis of novel conjugated polymers **P1**–**P7** containing 3,9-linked carbazole units in the main chain, and examined the optical and electrical properties. The polymers were obtained by the polycondensation of the corresponding diethynyl-substituted carbazole derivatives EEPCz and **8** with dihaloarenes (**1**–**7**) by the Sonogashira coupling polycondensation. The polymers were more soluble in various solvents than poly(3,9-carbazolyleneethynylenephenylene) that we previously synthesized. All the polymers absorbed light at a wavelength region longer than the carbazole units. This seems to be brought about by the conjugated main chain through the nitrogen atom of the carbazole unit. In addition, **P5**–**P7** exhibited absorption bands originating from charge transfer from carbazole to accepter units. The polymers emitted variously colored fluorescence excited at the main chain-based absorption maxima. Especially, **P1**, **P3** and **P3'** emitted blue fluorescence in high quantum yields. **P1**–**P3** were reversibly oxidized and reduced, whose oxidation potentials corresponded well with the λ_{max} values. **P3** showed the dark conductivity of 1.1×10^{-14} S/cm (10^3 V/cm).

Acknowledgment. This research was partly supported by a Grant-in-Aid for Science Research in a Priority Area ‘‘Super-Hierarchical Structures (No. 446)’’ from the Ministry of Education, Culture, Sports, Science and Technology, Japan.

References and Notes

[1] For reviews, see: (a) Grazulevicius JV, Strohriegl P, Pielichowski J, Pielichowski K. Prog Polym Sci 2003;28:1297; (b) Sasabe H. Supramol Sci 1996;3:91.

[2] For reviews, see: (a) Kippelen B, Meerholz K, Peyghambarian N. In Nonlinear Optics of Organic Molecules and Polymers; Nalwa HS, Miyata S, Eds. CRC Press: Boca Raton; 1997.pp. 465; (b) Kippelen B, Golemme A, Hendrickx E, Wang JF. : Marder S, Peyghambarian N. In Field Responsive Polymers: Electroresponsive, Photoresponsive, and Responsive Polymers in Chemistry and Biology; Khan IM, Harrison JS, Eds: ACS Symposium Series 726. Washington, DC: ACS; 1999 :pp. 204; (c) Wang YZ, Epstein A. J Acc Chem Res 1999;32:217.

[3] Morin JF, Leclerc M. Macromolecules 2002;35:8413.

[4] (a) Ngbilo E, Ades D, Chevrot C, Siove A. Polym Bull 1990;24:17;

(b) Faid K, Siove A, Ades D, Chevrot C. Synth Met 1993;55:1656;

(c) Zhang ZB, Fujiki M, Tang HZ, Motonaga M, Torimitsu K. Macromolecules 2002;35:1988;

(d) Iraqi A, Wataru I. J Polym Sci A Polym Chem 2004;42:6041.

[5] For recent reviews, see:

(a) Boudreault PLT, Blouin N, Leclerc M. Adv Polym Sci 2008;212:99;

(b) Blouin N, Leclerc M. Acc Chem Res 2008;41:1110.

[6] (a) Racchini JR, Wellinghoff ST, Schwab ST, Herrera CD, Jenekhe SA. Synth Met 1988;22:273;

(b) Grigalvicius S, Grazulevicius JV, Gaidelis V, Jankauskas V. Polymer 2002;43:2603.

[7] (a) Wu CW, Lin HC. Macromolecules 2006;39:7232;

(b) Liu R, Xiong Y, Zeng W, Wu Z, Du B, Yang W, Sun M, Cao Y. Macromol Chem Phys 2007;208:1503.

[8] (a) Bunz UHF. Chem Rev 2000;100:1605;

(b) Yamamoto T, Yamada W, Takagi M, Kizu K, Maruyama T. Macromolecules 1994;27:6620;

(c) Zhan X, Liu Y, Yu G, Wu X, Zhu D, Sun R, Wang D, Epstein AJ. J Mater Chem 2001;11:1606.

[9] Li H, Powell DR, Hayashi RK, West R. Macromolecules 1998;31:52.

[10] Takihana Y, Shiotsuki M, Sanda F, Masuda T. Macromolecules 2004;37:7578.

[11] Tamura K, Shiotsuki M, Kobayashi N, Masuda T, Sanda F. J Polym Sci A Polym Chem, accepted.

[12] Sanda F, Kawasaki R, Shiotsuki M, Takashima T, Fujii A, Ozaki M, Masuda T. Macromol Chem Phys 2007;208:765-771.

[13] Koehler DG, Liu D, De Feyter S, Enkelmann V, Weil T, Engels C, Samyn C, Mullen K, De Schryver FC. Macromolecules 2003;36:578-590.

[14] Mancilha FS, Neto BAD, Lopes AS, Moreira PFJ, Quina FH, Gonçalves RS, Dupont J. Eur J Org Chem 2006;4924–4933.

[15] (a) Jayakannan M, Van hal PA, Janssen RAJ. J Polym Sci A Polym Chem 2002;40:251-261;

(b) Hou Q, Xu Y, Yang W, Yuan M, Peng J, Cao Y. J Mater Chem 2002;12:2887–2892.

[16] Halgren TA. J Comput Chem 1996;17:490.

[17] (a) Zerner MC, Loew GH, Kirchner RF, Mueller-Westerhoff UT. J Am Chem Soc 1980;102:589;

(b) Ridley JE, Zerner MC. Theo Chim Acta 1973;32:111.

[18] For reviews see:

(a) Chinchilla R, Nájera C. Chem Rev 2007;107:874-922;

(b) Doucet H, Hierso J-C. Angew Chem Int Ed 2007;46:834–871.

[19] Kato S, Matsumoto T, Shigeiwa M, Gorohmaru H, Maeda S, Ishi-i T, Mataka S. Chem Eur J 2006;12:2303–2317.

[20] Feng D, Wang S, Zhuang Q, Guo P, Wu P, Han Z. J Mol Struct 2004;707:169-177.

[21] Zhang ZB, Fujiki M, Tang HZ, Motonaga M, Torimitsu K. Macromolecules 2002;35:1988-1990.

[22] Sanda F, Nakai T, Kobayashi N, Masuda T. Macromolecules 2004;37:2703.

Captions for Charts, Schemes and Figures

Chart 1. Structures of Poly(carbazole)s

Chart 2. Structure of Poly(3,9-carbazolyleneethynylenephenylene)

Scheme 1. Polycondensation of EEPCz and 8 with Dihaloarenes 1–7

Scheme 2. Synthetic Routes for EEPCz and 8

Figure 1. (a) UV-vis spectra of EEPCz and **P1**–**P3** (c = 1.70–3.43×10^{-5} M) and (b) **P4**–**P7** (c = 2.13–2.55×10^{-5} M) measured in THF.

Figure 2. UV-vis spectra of **8** and **P3'** (c = 1.99–2.92×10^{-5} M) measured in THF.

Figure 3. (a) UV-vis spectra of **P1** and **P2** predicted by MOS-F (ZINDO) and (b) relationship between the λ_{max} observed and predicted.

Figure 4. HOMO images of **P1** (top) and **P2** (bottom).

Figure 5. (a) Fluorescence spectra of EEPCz, **P1** and **P2** (c = 4.56–34.3×10^{-7} M), (b) **P3**–**P7** (c = 2.13–2.55×10^{-6} M), (c) **8** and **P3'** (c = 6.63–25.0×10^{-7} M) measured in THF. (d) Photograph of polymer solutions of **P3** and **P5**–**P7** (from left to right) under irradiation of UV light at 365 nm.

Figure 6. (a) UV-vis spectra (c = 2.74 × 10^{-5} M) and (b) fluorescence spectra (c = 4.56 × 10^{-7} M) of **P1** measured in various solvents.

Figure 7. UV-vis and fluorescence spectra of **P3** measured in the film state.

Figure 8. (a) UV-vis spectra of **P4** with irradiation at 300 < λ < 400 nm measured in THF (c = 2.13 × 10^{-5} M) and (b) with irradiation at 420 nm < λ, after irradiation at 300 < λ < 400 nm for 30 min.

Figure 9. (a) Cyclic voltammogram of **P1** (1 mM) measured at a scan rate of 0.1 V/s, vs Ag/Ag^+ in a n-Bu_4NClO_4 (0.1M) solution in CH_2Cl_2, 2nd–5th cycles. (b) Relationship between oxidation voltage (E_{ox}) determined by CV and λ_{max} of **P1**–**P3** together with EEPCz.

Figure 10. Relationships between current and voltage applied to ITO/**P3**/Au cells (effective electrode area 0.12 cm^2, thickness 20 μm) measured at room temperature under reduced pressure of 10^{-2} Torr. (■)Without photoirradiation. (●) Under photoirradiation (2.5 mW/m^2) with a Xe lamp using a thermoabsorption filter.

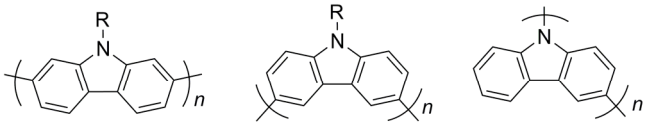

Poly(2,7-carbazole)s Poly(3,6-carbazole)s Poly(3,9-carbazole)

Chart 1. Structures of Poly(carbazole)s

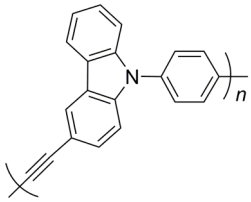

Chart 2. Structure of Poly(3,9-carbazolyleneethynylenephenylene)

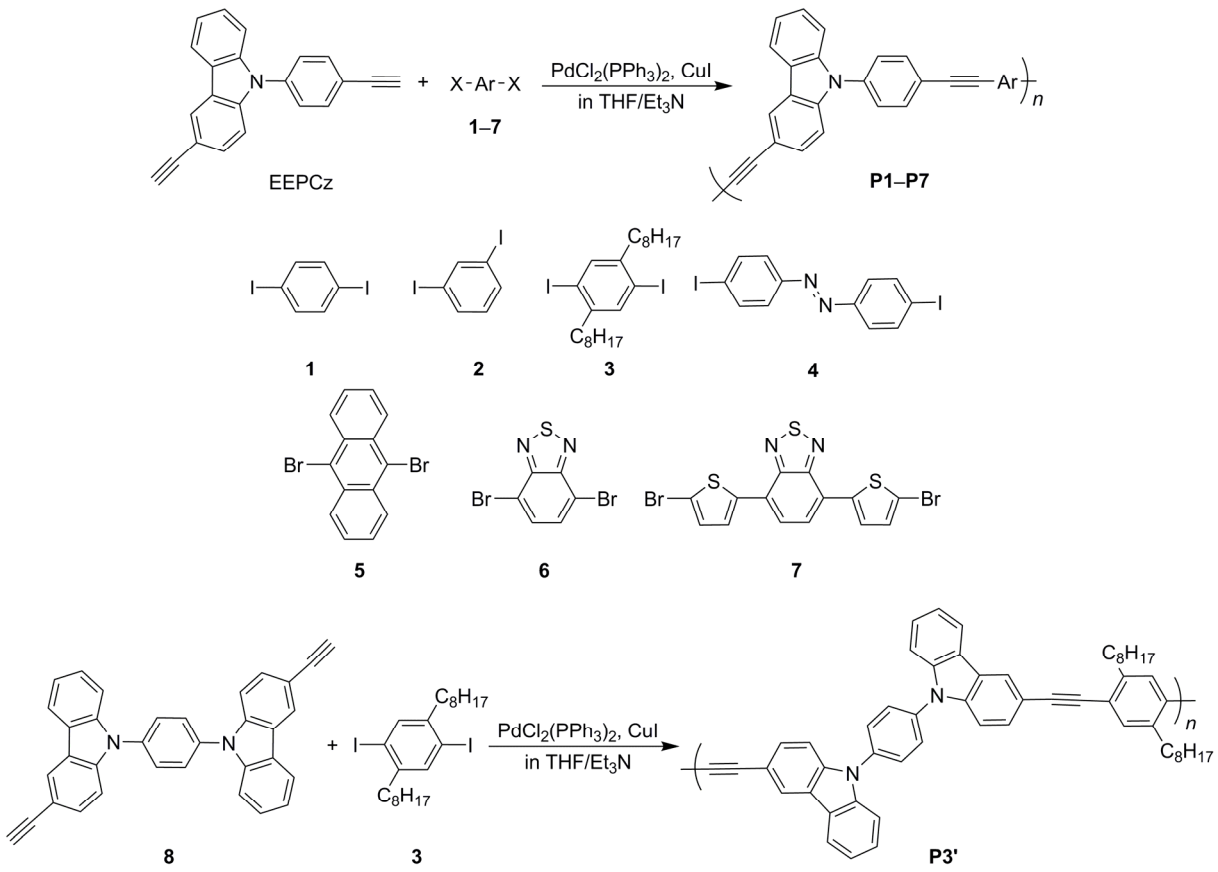

Scheme 1. Polycondensation of EEPCz and 8 with Dihaloarenes **1**–**7**

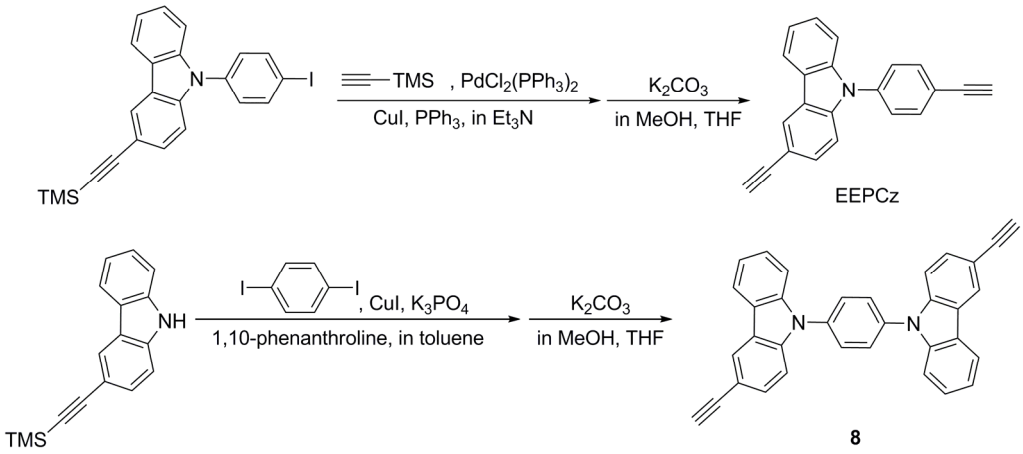

Scheme 2. Synthetic Routes for EEPCz and **8**

Table 1.
Polycondensation of EEPCz with Dihaloarenes **1–7** [a]

dihaloarene	temperature (°C)	polymer			
			yield [b] (%)	M_w	M_w/M_n [c]
1	30	**P1**	86	6 200	1.6
2	30	**P2**	85	4 100	1.4
3	30	**P3**	92	48 000	1.8
4	30	**P4**	57	12 500	2.2
5	50	**P5**	25	9 600	3.6
6	50	**P6**	24	8 400	2.6
7	50	**P7**	31	7 900	2.9

[a] Conditions: $[EEPCz]_0 = [dihaloarene]_0 = 0.10$ M, $[PdCl_2(PPh_3)_2] = 2.0$ mM, [CuI] = 8.0 mM, in THF/Et_3N = 4/1 (v/v), under N_2, 48 h.
[b] MeOH-insoluble part after filtration with THF.
[c] Estimated by GPC, eluent THF, (PSt standards).

Table 2.
Solubility of the Polymers [a]

	solvent						
polymer	hexane	toluene	CH_2Cl_2	$CHCl_3$	MeOH	acetone	DMF
P1	–	++	++	++	–	+	++
P2	–	++	++	++	–	+	++
P3	+	++	++	++	–	+	+
P4	–	+	+	++	–	+	+
P5	–	+	+	++	–	+	++
P6	–	+	+	++	–	+	+
P7	–	+	+	++	–	–	++
P3'	–	++	++	++	–	+	+
poly(3,9-carbazolyleneethynylenephenylene)	–	+	+	++	–	–	+

[a] THF-soluble part. Symbols: ++, soluble; +, partly soluble; –, insoluble.

Table 3.

UV-vis and Fluorescence Spectroscopic Data of the Polymers [a]

polymer	λ_{max} (nm)	λ_{emi} (nm)	ϕ [b] (%)
P1	303 355	400	91
P2	272 292 341	393	61
P3	304 361	399	83
P4	261 351 374	392	0.33
P5	290 355 374	499	63
P6	298 319 441	548	28
P7	320 478	566	22
P3'	303 347	392	80

[a] Measured in THF.

[b] Determined using anthracene as a standard.

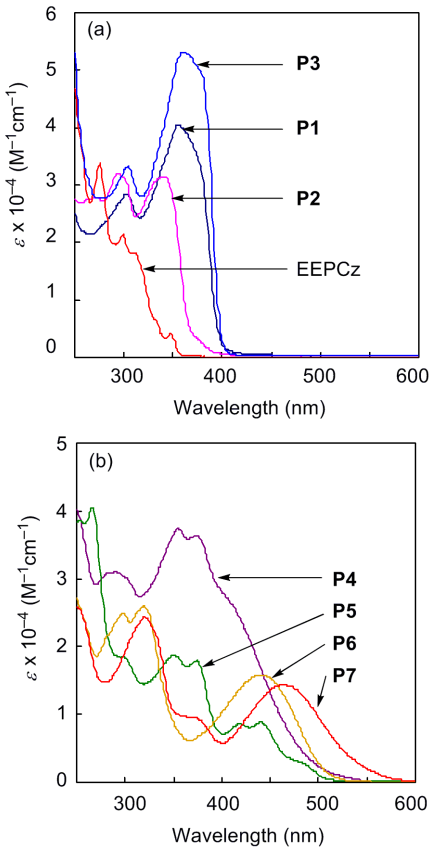

Figure 1. (a) UV-vis spectra of EEPCz and **P1**–**P3** (c = 1.70–3.43×10^{-5} M) and (b) **P4**–**P7** (c = 2.13–2.55×10^{-5} M) measured in THF.

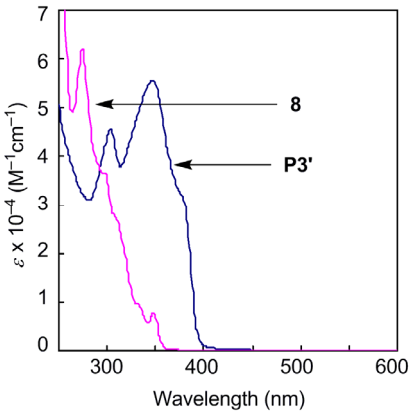

Figure 2. UV-vis spectra of **8** and **P3'** (c = 1.99–2.92×10^{-5} M) measured in THF.

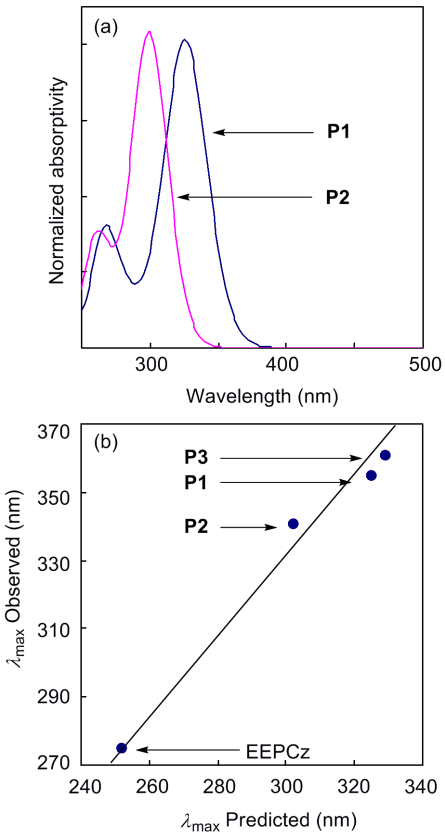

Figure 3. (a) UV-vis spectra of **P1** and **P2** predicted by MOS-F (ZINDO) and (b) relationship between the λ_{max} observed and predicted.

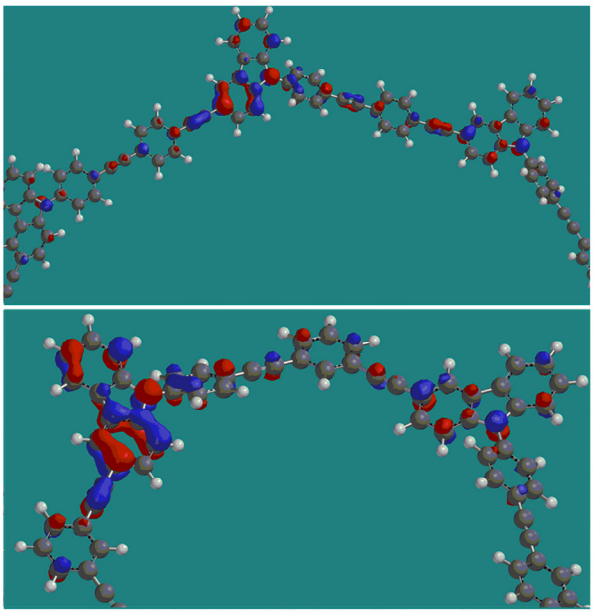

Figure 4. HOMO images of **P1** (top) and **P2** (bottom).

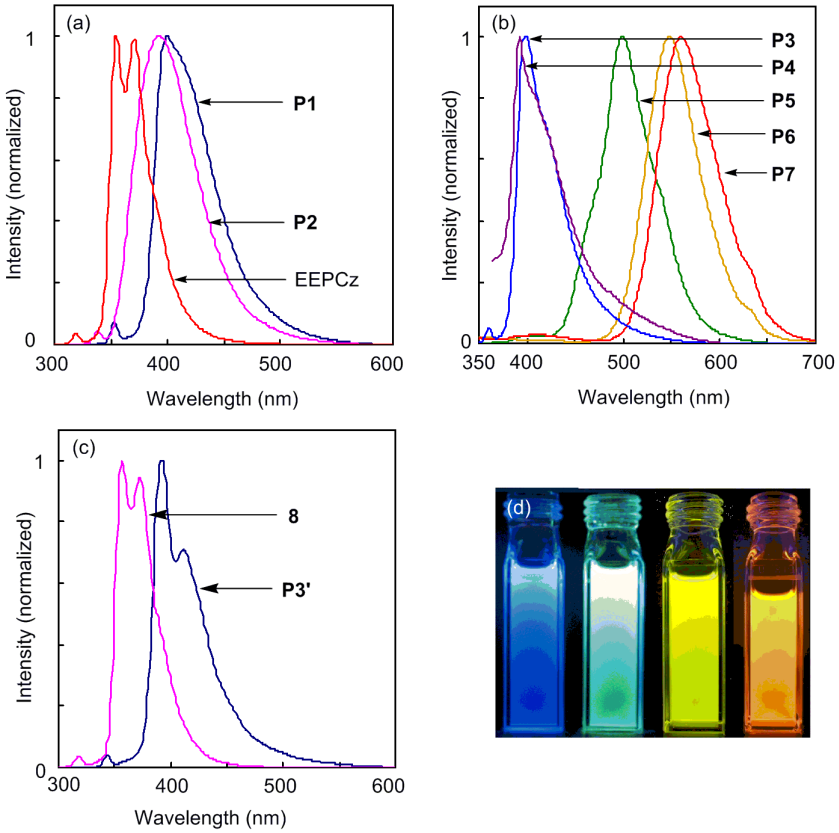

Figure 5. (a) Fluorescence spectra of EEPCz, **P1** and **P2** (c = 4.56–34.3×10^{-7} M), (b) **P3**–**P7** (c = 2.13–2.55×10^{-6} M), (c) **8** and **P3'** (c = 6.63–25.0×10^{-7} M) measured in THF. (d) Photograph of polymer solutions of **P3** and **P5**–**P7** (from left to right) under irradiation of UV light at 365 nm.

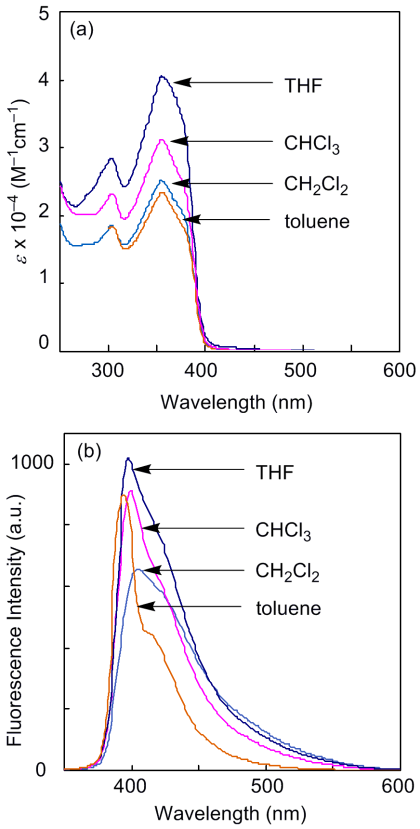

Figure 6. (a) UV-vis spectra ($c = 2.74 \times 10^{-5}$ M) and (b) fluorescence spectra ($c = 4.56 \times 10^{-7}$ M) of **P1** measured in various solvents.

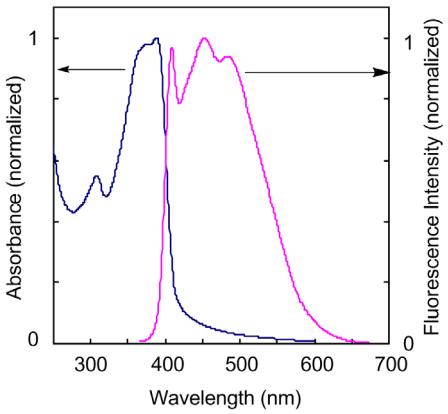

Figure 7. UV-vis and fluorescence spectra of **P3** measured in the film state.

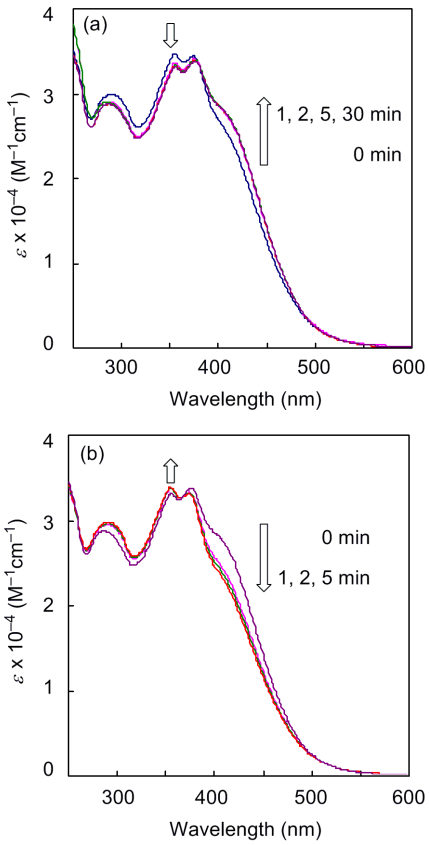

Figure 8. (a) UV-vis spectra of **P4** with irradiation at $300 < \lambda < 400$ nm measured in THF (c = 2.13×10^{-5} M) and (b) with irradiation at 420 nm < λ, after irradiation at $300 < \lambda < 400$ nm for 30 min.

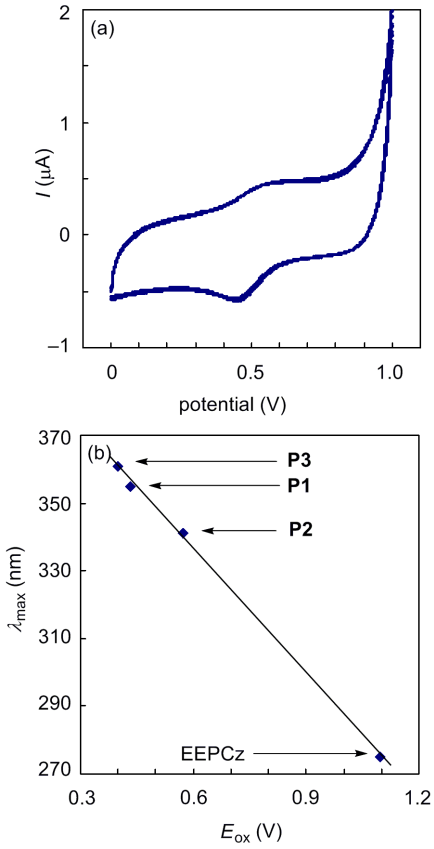

Figure 9. (a) Cyclic voltammogram of **P1** (1 mM) measured at a scan rate of 0.1 V/s, vs Ag/Ag^+ in a *n*-Bu_4NClO_4 (0.1M) solution in CH_2Cl_2, 2nd–5th cycles. (b) Relationship between oxidation voltage (E_{ox}) determined by CV and λ_{max} of **P1**–**P3** together with EEPCz.

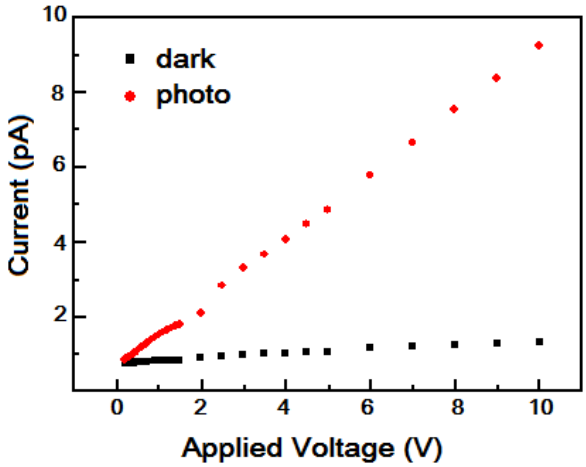

Figure 10. Relationships between current and voltage applied to ITO/**P3**/Au cells (effective electrode area 0.12 cm^2, thickness 20 μm) measured at room temperature under reduced pressure of 10^{-2} Torr. (■)Without photoirradiation. (●) Under photoirradiation (2.5 mW/m^2) with a Xe lamp using a thermoabsorption filter.